

# Coupling of Terminal Alkynes and Isonitriles by Organoactinide Complexes: Scope and Mechanistic Insights

Eyal Barnea,<sup>†</sup> Tamer Andrea,<sup>†</sup> Jean-Claude Berthet,<sup>‡</sup> Michel Ephritikhine,<sup>‡</sup> and Moris S. Eisen<sup>\*†</sup>

Schulich Faculty of Chemistry and Institute of Catalysis Science and Technology, Technion—Israel Institute of Technology, Haifa 32000, Israel, and Service de Chimie Moléculaire, DSM/IRAMIS, Laboratoire Claude Fréjacques, CNRS URA 331, CEA Saclay, Gif-sur-Yvette Cedex 91191, France

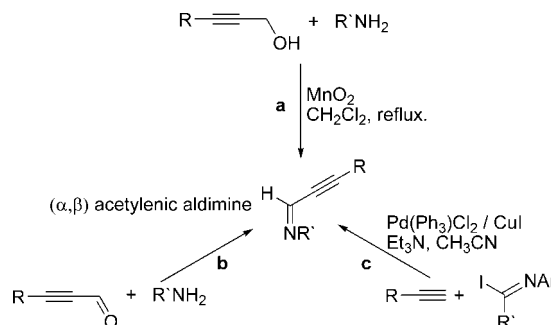
Received December 6, 2007

The coupling reaction of terminal alkynes with several isocyanides, catalyzed by the neutral organoactinide complexes  $\text{Cp}^*_2\text{AnMe}_2$  ( $\text{Cp}^* = \text{C}_5\text{Me}_5$ ,  $\text{An} = \text{Th}, \text{U}$ ) or the cationic complex  $[(\text{Et}_2\text{N})_3\text{U}][\text{BPh}_4]$ , yielded substituted  $\alpha,\beta$ -acetylenic aldimines, in good to excellent yields. The reaction proceeded via a 1,1-insertion of the isocyanide carbon into a metal–acetylide bond, followed by a protonolysis by the acidic proton of the terminal alkyne. Additional insertion products were obtained by altering the catalyst and the reactant ratios. A plausible mechanism for the catalytic reaction is also presented, based on kinetics measurements and thermodynamic studies of the coupling reaction with  $\text{Cp}^*_2\text{ThMe}_2$  or  $[(\text{Et}_2\text{N})_3\text{U}][\text{BPh}_4]$  as catalysts. The reaction is first-order in catalyst and isocyanide and zero-order in alkyne.

## Introduction

During the last decade, the interest in the catalytic activity of actinides has been increasing due to their rich, complex, and unique chemistry.<sup>1–4</sup> However, in all of the previous studies, for all the processes, the main activation pathway followed a four-center transition state. Hence we find it conceptually challenging and interesting to investigate the reactivity of this family of organo-f-complexes in other catalytic processes, such as the coupling of terminal alkynes with isocyanides to produce  $\alpha,\beta$ -acetylenic aldimines (Scheme 1), which is expected to proceed through a three-center transition state. The ability to succeed in such transitions opens the scope of reactivity for organo-f-complexes.  $\alpha,\beta$ -Acetylenic aldimines are attractive molecules for organic synthesis and are used as starting synthons for elaborated synthesis. For example, the recent methodology for the synthesis of 2-(propargylamino)ethanols, in a one-pot

## Scheme 1. Methods for the Preparation of $\alpha,\beta$ -Acetylenic aldimines



synthesis, excluding the isolation of unstable (prop-2-ynylideneamino)ethanols was developed.<sup>5</sup> The  $\alpha,\beta$ -acetylenic aldimines contain four different functional groups (basic nitrogen moiety, carbon–nitrogen double bond, carbon–carbon triple bond, and a propargylic substituent that can be a functional group such as silicon, olefinic moiety, and others) that shape the desirable polyfunctionality and versatility of this synthon. These compounds can be synthesized by three main reactions (Scheme 1). The first reaction (Scheme 1, pathway a) involves a propargyl alcohol and an amine in the presence of an oxidizing agent such as  $[\text{MnO}_2]$ .<sup>6</sup> The second route (Scheme 1, pathway b) involves the condensation of propynals with aliphatic and aromatic amines.<sup>7</sup> The third methodology (Scheme 1, pathway c) involves a Pd-catalyzed cross-coupling reaction of a terminal alkyne with an iodoimine.<sup>8</sup>

Isonitriles ( $\text{RN}\equiv\text{C}:$ ) are two-electron-donor ligands that are known to undergo a 1,1-insertion, under stoichiometric condi-

\* chmoris@tx.technion.ac.il.

<sup>†</sup> Technion—Israel Institute of Technology.

<sup>‡</sup> CNRS URA 331.

(1) For examples of catalytic activity of organoactinides in hydrogenation of olefins see: (a) Eisen, M. S.; Marks, T. J. *J. Am. Chem. Soc.* **1992**, *114*, 10358–68. (b) Lin, Z.; Marks, T. J. *J. Am. Chem. Soc.* **1990**, *112*, 5515–25. (c) Gillespie, R. D.; Burwell, R. L.; Marks, T. J. *Langmuir* **1990**, *6*, 1465–77.

(2) For examples of catalytic activity of organoactinides in oligomerizations, or controlled dimerizations, of terminal alkynes see: (a) Wang, J.; Dash, A. K.; Kapon, M.; Berthet, J. C.; Ephritikhine, M.; Eisen, M. S. *Chem.—Eur. J.* **2002**, *8*, 5384–96. (b) Wang, J. Q.; Dash, A. K.; Berthet, J. C.; Ephritikhine, M.; Eisen, M. S. *Organometallics* **1999**, *18*, 2407–09. (c) Haskel, A.; Straub, T.; Dash, A. K.; Eisen, M. S. *J. Am. Chem. Soc.* **1999**, *121*, 3014–24. (d) Dash, A. K.; Wang, J. X.; Berthet, J. C.; Ephritikhine, M.; Eisen, M. S. *J. Organomet. Chem.* **2000**, *604*, 83–98. (e) Haskel, A.; Wang, J. Q.; Straub, T.; Neyroud, T. G.; Eisen, M. S. *J. Am. Chem. Soc.* **1999**, *121*, 3025–34.

(3) For recent examples of catalytic activity of organoactinides in hydroamination, see ref 2a and: (a) Stubbert, B. D.; Marks, T. J. *J. Am. Chem. Soc.* **2007**, *129*, 4253–71. (b) Stubbert, B. D.; Stern, C. L.; Marks, T. J. *Organometallics* **2003**, *22*, 4836–38. (c) Straub, T.; Haskel, A.; Neyroud, T. G.; Kapon, M.; Botoshansky, M.; Eisen, M. S. *Organometallics* **2001**, *20*, 5017–35.

(4) (a) Dash, A. K.; Gourevich, I.; Wang, J. Q.; Wang, J.; Kapon, M.; Eisen, M. S. *Organometallics* **2001**, *20*, 5084–104. (b) Barnea, E.; Moradove, D.; Berthet, J. C.; Ephritikhine, M.; Eisen, M. S. *Organometallics* **2006**, *25*, 320–322.

(5) (a) Karpov, M. V.; Khranchikhin, A. V.; Suvorova, I. V.; Pitserskaya, Y. L.; Stadnichuk, M. D. *Russ. J. Gen. Chem.* **2007**, *77*, 899–904. (b) Stadnichuk, M. D.; Khranchikhin, A. V.; Pitserskaya, Y. L.; Suvorova, I. V. *Russ. J. Gen. Chem.* **1999**, *69*, 593–609.

(6) Blackburn, L.; Taylor, R. J. K. *Org. Lett.* **2001**, *3*, 1637–39, and references therein.

(7) Hachiya, I.; Ogura, K.; Shimizu, M. *Org. Lett.* **2002**, *4*, 2755–57, and references therein.

(8) Uneyama, K.; Watanabe, H. *Tetrahedron Lett.* **1991**, *32*, 1459–62.

tions, into a metal–acetylide bond of an early or a late transition metal complex, but this has never been evaluated for organo-5f-elements.<sup>9a</sup> The reactivity of the isonitrile molecules is a result of the lone pair of electrons, as in carbenes. In 1998 Erker et al.<sup>10</sup> reported that the cationic metallocene-acetylide complexes of group IV metals undergo insertion of isonitriles into the metal–acetylide bond. However, this reaction was performed on a stoichiometric ratio, and no data were presented regarding the possibility for a catalytic reaction.<sup>11</sup> Another example was presented by Takahashi et al. using the heterodinuclear  $\mu$ -ethynediyl complex  $\text{Cl}(\text{R}_3\text{P})_2\text{Pt}-\text{C}\equiv\text{C}-\text{Pd}(\text{PR}_3)_2\text{Cl}$ , which, with an excess of arylisonitrile, affords multiple isonitrile insertions into the Pd–acetylide bond to form polyisonitriles.<sup>12</sup> Odom et al. has elegantly designed a three-component coupling of terminal alkynes, isonitriles, and primary amines or hydrazines, catalyzed by titanium complexes, to form  $\alpha,\beta$ -unsaturated- $\beta$ -iminoamines or  $\alpha,\beta$ -unsaturated- $\beta$ -hydrazonylimines.<sup>13</sup> In this contribution we report on the catalytic coupling reaction between isonitriles and terminal alkynes promoted by organoactinides. We show the crucial effect of the metal toward a specific product, which eventually shows the unique reactivity of actinides as compared to early or late transition complexes. In addition we present kinetics and thermodynamic studies that allow us to propose a plausible mechanism for each complex in these reactions. The data obtained can be used to compare the reactivity of different substrates toward a specific complex with its respective ancillary ligand to tailor future catalytic processes.

## Results and Discussion

The organoactinide complexes  $\text{Cp}^*_2\text{AnMe}_2$  [ $\text{Cp}^* = \text{C}_5\text{Me}_5$ ,  $\text{An} = \text{Th}$  (**1**),  $\text{U}$  (**2**)] and the cationic complex  $[(\text{Et}_2\text{N})_3\text{U}][\text{BPh}_4]$  (**3**) were found to be active catalysts for the coupling of isonitrile and terminal alkynes (eqs 1–3), via a 1,1-insertion of the isonitrile terminal carbon atom into a metal–acetylide or a metal–imine bond.<sup>14,15</sup> The complete conversion of the isonitrile and alkyne to 1-aza-1,3-enynes was achieved in benzene or toluene at 60–100 °C, while no reaction was observed in the absence of catalyst. The product distribution for the coupling reaction was found to depend strongly on both the catalyst and the alkyne:isonitrile ratio.

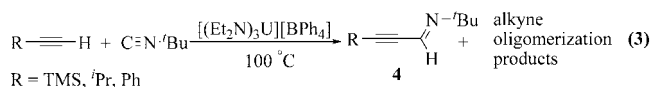
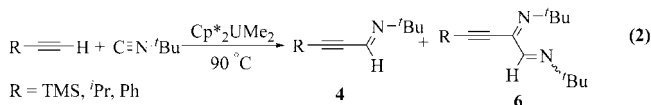
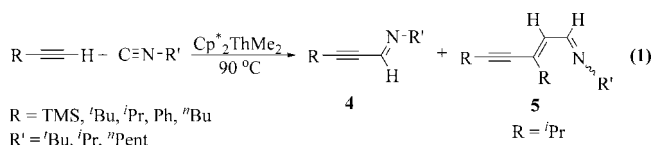
The reaction between bulky terminal alkynes ( $\text{R} = \text{TMS}$ ,  $^t\text{Bu}$ ,  $\text{Ph}$ ) and  $^t\text{BuN}\equiv\text{C}$  in the presence of complex **1** (Table 1, entries 1–6) produces compound **4** (eq) as the only product, even with an excess of alkyne. The reaction was monitored by  $^1\text{H}$  NMR,

**Table 1.** Data for the Coupling of Terminal Alkynes ( $\text{RC}\equiv\text{CH}$ ) with Isonitriles ( $\text{R}'\text{N}\equiv\text{C}$ ) Catalyzed by Complex **1**

entry	R'	R	R'N≡C: RC≡CH <sup>a</sup>	time (h)	<b>4</b> (%) <sup>b</sup>	<b>5</b> (%) <sup>b</sup>
1	$^t\text{Bu}$	TMS	100:100	23	90	
2	$^t\text{Bu}$	TMS	100:180	3	35	
3	$^t\text{Bu}$	TMS	100:180	18	85	
4	$^t\text{Bu}$	$^t\text{Bu}$	100:100	18	80	
5	$^t\text{Bu}$	$^t\text{Bu}$	100:200	18	90	
6	$^t\text{Bu}$	Ph	100:100	20	90	
7	$^t\text{Bu}$	$^i\text{Pr}$	100:100	18	90	
8	$^t\text{Bu}$	$^i\text{Pr}$	100:200	2	19	0
9	$^t\text{Bu}$	$^i\text{Pr}$	100:200	17	95	5
10	$^t\text{Bu}$	$^i\text{Pr}$	100:200	64	60	40
11	$^t\text{Bu}$	$^i\text{Pr}$	100:200	210	47	53
12	$^t\text{Bu}$	$^n\text{Bu}$	100:50	4	28	
13	$^t\text{Bu}$	$^n\text{Bu}$	100:50	17	N/A <sup>c</sup>	
14	$^i\text{Pr}$	TMS	100:100	4	84 (Z) <sup>c</sup>	
15	$^i\text{Pr}$	$^t\text{Bu}$	100:100	4	77	
16	$^i\text{Pr}$	Ph	100:100	5	82	
17	$^n\text{Pent}$	TMS	100:100	0.5	95 <sup>d</sup>	
18	$^n\text{Pent}$	$^n\text{Bu}$	200:200	5	90 <sup>d</sup>	
19	$^n\text{Pent}$	Ph	100:100	5	89 <sup>d</sup>	

<sup>a</sup> Relative to 1 equiv of catalyst. <sup>b</sup> Measured by  $^1\text{H}$  NMR. <sup>c</sup> See text.

<sup>d</sup> A mixture of both *E* and *Z* isomers (see text).



as can be seen in Figure 1 for the reaction of  $\text{TMSC}\equiv\text{CH}$  (excess) with  $^t\text{BuN}\equiv\text{C}$  (entry 2 in Table 1). As the reaction progresses, the signals of the acetylenic proton (**a**), TMS protons (**b**), and  $^t\text{BuN}\equiv\text{C}$  protons (**c**) decrease with the increase in product signals (aldimine proton (**e**), TMS (**d**), and *tert*-butyl group (**f**)).

NOE studies of the products showed space proximity between the  $\text{R}'$  group and the imine hydrogen. Hence, it can be deduced that these two groups are positioned *syn* to each other, producing the imine moiety with an *E* configuration. Computational calculations of  $\Delta E_0$  for the reaction of  $^t\text{BuN}\equiv\text{C}$  and  $\text{TMSC}\equiv\text{CH}$  show that the reaction to produce the monocoupling *E* product, **4** ( $\Delta E_0 = -17.6$  kcal/mol), is thermodynamically favorable as compared to the production of the *Z* isomer ( $\Delta E_0 = -14.5$  kcal/mol).<sup>16</sup>

When the smaller  $^i\text{PrC}\equiv\text{CH}$  reacts in a 1:1 ratio with  $^t\text{BuN}\equiv\text{C}$  (entry 7), the reaction produces only product **4**. However, when the reaction was performed with an excess of  $^i\text{PrC}\equiv\text{CH}$  (entries

(9) For preliminary communication, see: (a) Barnea, E.; Andrea, T.; Kapon, M.; Berthet, J.-C.; Ephritikhine, M.; Eisen, M. S. *J. Am. Chem. Soc.* **2004**, *126*, 10860–10861. (b) Takei, F.; Yanai, K.; Onitsuka, K.; Takahashi, S. *Chem.-Eur. J.* **2000**, *6*, 983–993.

(10) Ahlers, W.; Erker, G.; Fröhlich, R. *J. Organomet. Chem.* **1998**, *571*, 83–89.

(11) (1) For an example of isonitrile insertion into a Ti–alkyl bond see: Martins, A. M.; Ascenso, J. R.; De-Azevedo, C. G.; Dias, A. R.; Duarte, M. T.; Da-Silva, J. F.; Veiros, L. F.; Rodrigues, S. S. *Organometallics* **2003**, *22*, 4218–4228.

(12) Onitsuka, K.; Yanai, K.; Takei, F.; Joh, T.; Takahashi, S. *Organometallics* **1994**, *13*, 3862–3867.

(13) (a) Banerjee, S.; Shi, Y.; Cao, C.; Odom, A. L. *J. Organomet. Chem.* **2005**, *690*, 5066–77. (b) Cao, C.; Shi, Y.; Odom, A. L. *J. Am. Chem. Soc.* **2003**, *125*, 2880–81. (c) Barnea, E.; Moradove, D.; Berthet, J. C.; Ephritikhine, M.; Eisen, M. S. *Organometallics* **2006**, *25*, 320–22.

(14) For a review on 1,1-insertions into a metal–carbon bond see: Kayaki, Y.; Yamamoto, A. *Curr. Meth. Inorg. Chem.* **2003**, *3*, 373–409.

(15) Stoichiometric 1,1-insertion of isonitriles into an actinide–carbon bond was reported. See: (a) Dormond, A.; Aaliti, A.; Elbouadili, A.; Moise, C. *J. Organomet. Chem.* **1987**, *329*, 187–199. (b) Moloy, K. G.; Fagan, P. J.; Manriquez, J. M.; Marks, T. J. *J. Am. Chem. Soc.* **1986**, *108*, 56–67.

(16) The geometries of all molecules were optimized using the hybrid B3LYP density functional method with the 6-311G(d,p) basis set. Vibrational frequencies were calculated at this level of theory for all stationary points, in order to verify them as minima. Real vibrational frequencies confirmed the presence of minima on the potential energy surface. All energies discussed in this work include zero-point vibration correction (i.e., B3LYP/6-311G(d,p)+ZPVE).

(17) (a) Manriquez, J. M.; Fagan, P. J.; Marks, T. J. *J. Am. Chem. Soc.* **1978**, *100*, 3939–41. (b) Bruno, J. W.; Smith, G. M.; Marks, T. J.; Fair, C. K.; Schultz, A. J.; Williams, J. M. *J. Am. Chem. Soc.* **1986**, *108*, 40–56.

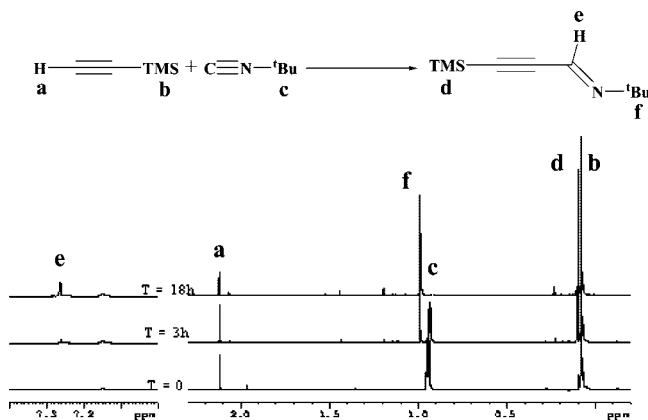


**Figure 1.**  $^1\text{H}$  NMR monitoring of the reaction of  $\text{TMSC}\equiv\text{CH}$  with  $^t\text{BuN}\equiv\text{C}$  catalyzed by complex **1** (entry 2 in Table 1).

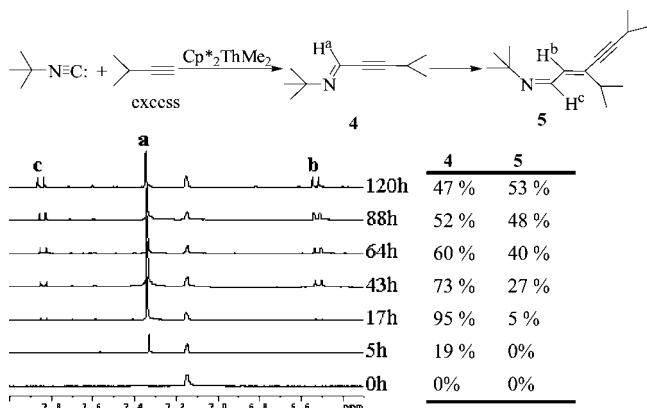


**Figure 2.**  $^1\text{H}$  NMR monitoring of the reaction of  $^i\text{PrC}\equiv\text{CH}$  with  $^t\text{BuN}\equiv\text{C}$  catalyzed by complex **1**, showing the formation of product **5**.

8–11) as a function of time, the formation of the additional product **5** was observed, by both  $^1\text{H}$  NMR and GC-MS. Figure 2 shows the progress of the reaction as monitored by  $^1\text{H}$  NMR. The signal of the aldiminic proton of **4** (**a**) reaches a maximum after 17 h. From that time, the amount of compound **4** decreases, and the amount of compound **5** (seen as the vinyl proton **b** and the imine proton **c**) increases up to a steady state where the ratio of **4** to **5** is nearly 1:1. The variation of the molar ratio of **4** and **5** over time suggests that **5** is formed only after the complete formation of **4** (no more isonitrile is present in the reaction mixture), by its reaction with the remaining alkyne. The addition of more alkyne induces the full conversion of compound **4** into **5** selectively. The formation of **5** was also achieved by addition of alkyne to a solution of compound **4** and catalyst (without added isonitrile) at 80 °C. Nearly quantitative amounts of **5** were obtained via this method.

The reaction of  $^n\text{BuC}\equiv\text{CH}$  with  $^t\text{BuN}\equiv\text{C}$  (in a 1:2 ratio) also afforded the corresponding product **4** in 28% yield after 4 h (entries 12, 13 in Table 1). Longer reaction times resulted in the formation of many byproducts. The mixture was analyzed by GC-MS and was found to include the corresponding compounds **4** and **5** as well as a myriad of unidentified products, containing one and two acetylene moieties and up to three isonitrile molecules. Using equimolar amounts of isonitrile and alkyne produces compound **4** in lower amounts after 4 h, and the mixture of compounds is already present at low conversions. This result suggests that for the nonbulky  $^n\text{BuC}\equiv\text{CH}$ , parallel

pathways are operative other than that for the formation of the major product **4**.

The reaction of several terminal alkynes with  $^i\text{PrN}\equiv\text{C}$  and  $^n\text{PentN}\equiv\text{C}$  were also studied (entries 14–19). As can be seen, these reactions proceed to completion faster than with  $^t\text{BuN}\equiv\text{C}$ , probably due to the smaller steric hindrance for the approach of the isonitrile to the metal center. The reaction of  $\text{TMSC}\equiv\text{CH}$  with  $^i\text{PrN}\equiv\text{C}$  afforded the clean *Z* isomer after 4 h (entry 14). However, longer heating times resulted in the isomerization of this product to the more stable *E* isomer. Hence, it seems plausible to conclude that the *Z* isomer is the kinetic product of the coupling reaction, whereas the *E* isomer is the stable thermodynamic product. This transformation is catalyzed by the actinide complex; however the same isomerization can be obtained from the clean *Z* product at prolonged amounts of time or at higher temperatures. Interestingly, similar behavior was observed for the reaction of all terminal alkynes with  $^n\text{PentN}\equiv\text{C}$ . For example, the reaction with  $\text{TMSC}\equiv\text{CH}$  (entry 17) came to completion after 30 min at 90 °C, forming a mixture of both *E* and *Z* isomers (with *Z*:*E* ratio of 2.5:1). After an additional 24 h at 90 °C partial isomerization of the *Z* isomer to the *E* isomer was observed (final *Z*:*E* ratio of 1:1.8).

The influence of the steric hindrance of the isonitrile on the reaction was tested by following a competing reaction using an equimolar mixture of  $^t\text{BuN}\equiv\text{C}$  and  $^n\text{PentN}\equiv\text{C}$  with excess  $\text{TMSC}\equiv\text{CH}$ . We have found that the alkyne reacts with the less bulky isonitrile first. Only after the complete consumption of the  $^n\text{PentN}\equiv\text{C}$  does the excess alkyne react with the bulkier  $^t\text{BuN}\equiv\text{C}$ .

**Kinetics Studies on the Coupling of  $\text{TMSC}\equiv\text{CH}$  and  $^t\text{BuN}\equiv\text{C}$  Catalyzed by  $\text{Cp}^*_2\text{ThMe}_2$  and  $[(\text{Et}_2\text{N})_3\text{U}][\text{BPh}_4]$ .** In order to propose a plausible mechanism for the coupling reaction and learn about the alkyne, isonitrile, catalyst, and temperature influence on the reaction rate, kinetics measurements were conducted. Kinetics studies of the  $\text{Cp}^*_2\text{ThMe}_2$ - and  $[(\text{Et}_2\text{N})_3\text{U}][\text{BPh}_4]$ -catalyzed coupling of  $\text{TMSC}\equiv\text{CH}$  and  $^t\text{BuN}\equiv\text{C}$  in benzene- $d_6$  were carried out and followed by in situ  $^1\text{H}$  NMR spectroscopy. The strong and clear signal at  $\delta$  0.05 of the nine hydrogen atoms of the alkyne TMS group gradually disappeared with the course of the reaction and a new signal simultaneously appears as a singlet at  $\delta$  0.11, corresponding to the TMS group of the coupling product. The same process can also be followed via the disappearance of the isonitrile's  $^t\text{Bu}$  protons (at  $\delta$  0.96) and the appearance of the product's  $^t\text{Bu}$  group (at  $\delta$  1.05) or the appearance of the imine proton (at  $\delta$  7.26). These signals were used for monitoring the concentration changes taking place as the result of the reaction using  $^1\text{H}$  NMR (Figure 3).

**Influence of  $\text{Cp}^*_2\text{ThMe}_2$  Concentration on the Reaction Rate.** Different concentrations of catalyst, within a 10-fold range, were used while alkyne and isonitrile concentrations were kept constant. The kinetics of the coupling were monitored using the intensity changes in the substrate and product resonances over 3 or more half-lives. The rate constant,  $k_{\text{obs}}$  ( $\text{M}\cdot\text{s}^{-1}$ ), was calculated from the linear part of the plot showing the product concentration versus time. The results are presented in Figure 4, showing a graphic representation of the results;  $k_{\text{obs}}$  exhibits a linear increase with the increase of the catalyst concentration. Thus,  $k_{\text{obs}}$  as a function of the catalyst concentration follows first-order behavior.

**Influence of Isonitrile Concentration on the Reaction Rate.** The concentration of  $^t\text{BuN}\equiv\text{C}$  was varied also, over a 10-fold range, while catalyst and alkyne concentrations were kept constant. The kinetics of the coupling reaction were

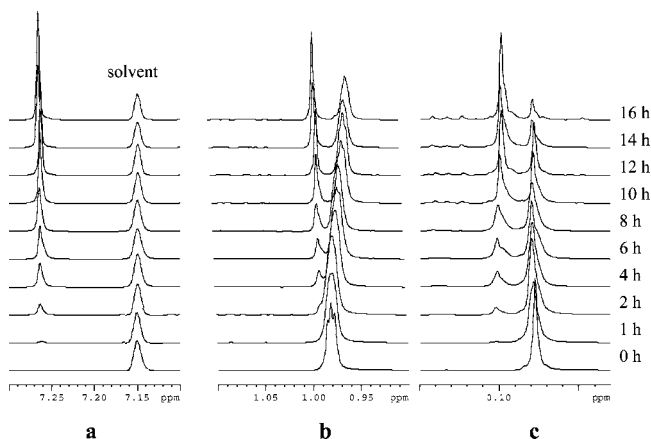


**Figure 3.** Formation of  $\text{TMSC}\equiv\text{C(H)=N'Bu}$ , followed by  $^1\text{H}$  NMR in the general reaction: (a) imine (and solvent) region, (b) 'B group region, (c) TMS group region.

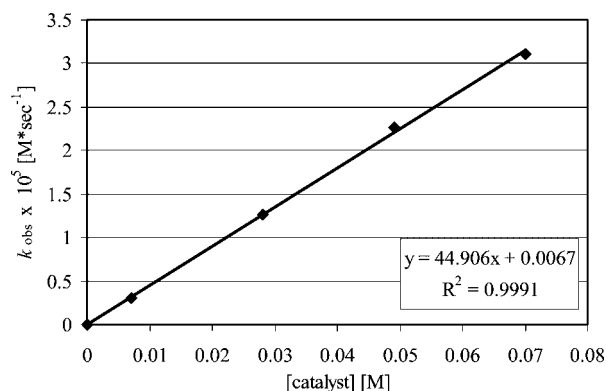


**Figure 4.** Dependence of  $k_{\text{obs}}$  on  $\text{Cp}^*_2\text{ThMe}_2$  concentration ([alkyne] = 2 M, [isonitrile] = 2 M, temp = 80 °C).

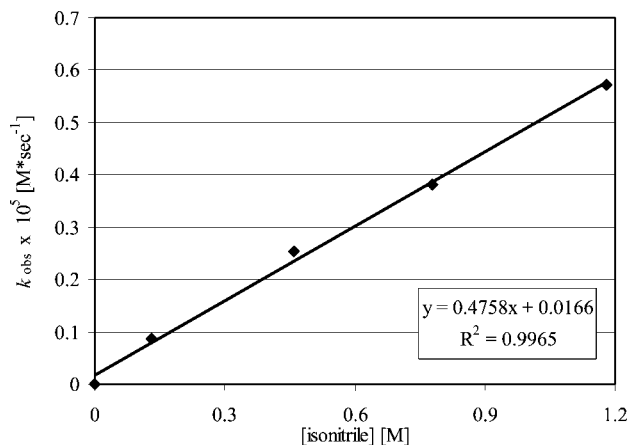


**Figure 5.** Dependence of  $k_{\text{obs}}$  on isonitrile concentration ([alkyne] = 2 M, [complex **1**] = 0.02 M, temp = 80 °C).

monitored as shown before over 3 or more half-lives. The results are presented in Figure 5. The graphic representation of  $k_{\text{obs}}$  as a function of isonitrile concentration yields a linear plot, indicating the first-order kinetics dependence on the  $t\text{BuN}\equiv\text{C}$  concentration.

**Influence of  $\text{TMSC}\equiv\text{CH}$  Concentration on the Reaction Rate.** The concentration of  $\text{TMSC}\equiv\text{CH}$  was varied, over a 10-fold range, while the catalyst and the isonitrile concentrations were kept constant. The kinetics of the coupling reaction were monitored as indicated for the catalysts and the

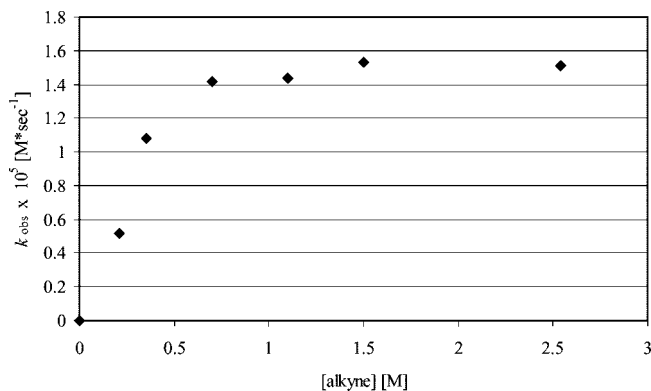


**Figure 6.** Dependence of  $k_{\text{obs}}$  on the  $\text{TMSC}\equiv\text{CH}$  concentration ([isonitrile] = 2 M, [complex **1**] = 0.02 M, temp = 80 °C).

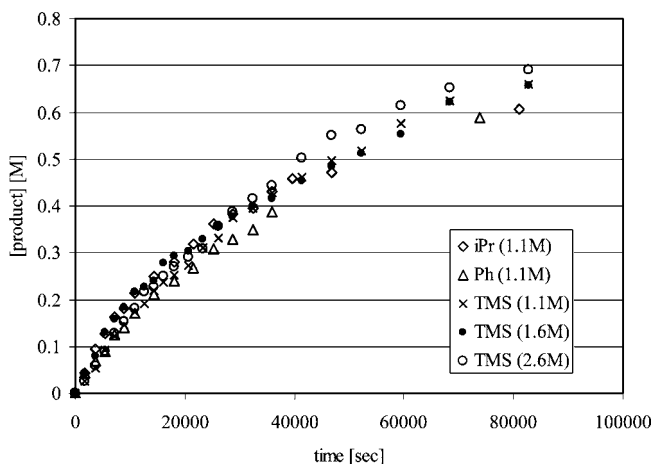


**Figure 7.** Product concentration over time for several terminal alkynes ([isonitrile] = 2 M, [complex **1**] = 0.02 M, temp = 80 °C).

isonitrile. The measured rate constants,  $k_{\text{obs}}$  ( $\text{M}\cdot\text{s}^{-1}$ ), was calculated as before, and the results are presented in Figure 6.

As can be seen from Figure 6,  $k_{\text{obs}}$  as a function of alkyne concentration seems to follow two domains. At low concentrations, first-order kinetics are followed, whereas at high concentrations, zero-order kinetics are exhibited. As was mentioned earlier, under alkyne starvation, oligomerization of isonitrile (i.e., insertion of a second or third isonitrile) competes with the product formation. We therefore consider that the decrease in  $k_{\text{obs}}$  for low alkyne concentration is a result of such side reactions. To verify that the reaction is indeed zero-order in alkyne, we have tested the effect of changing the alkyne on kinetics (Figure 7). We have found that changing the alkyne from  $\text{TMSC}\equiv\text{CH}$  to  $\text{PhC}\equiv\text{CH}$  or  $i\text{PrC}\equiv\text{CH}$  (all of them with different electronic and steric parameters) did not affect the rate of reaction. Thus we can conclude that the kinetic rate law is of zero-order for the alkyne concentration.

The combined data obtained in the experiments described above allow us to express the kinetics equation, which the coupling of isonitrile and alkynes follows under the catalytic effect of complex **1** (eq 4).

$$v = k[\text{complex } \mathbf{1}]^1[t\text{BuN}\equiv\text{C}]^1[\text{TMSC}\equiv\text{CH}]^0 \quad (4)$$

This leads to the conclusion that the rate-determining step is the insertion of the isonitrile into the metal–acetylide bond. Because oxidation of Th(IV) is energetically unfavorable, the insertion of the isonitrile at the rate-determining step must undergo formation of a three-center transition state, as expected



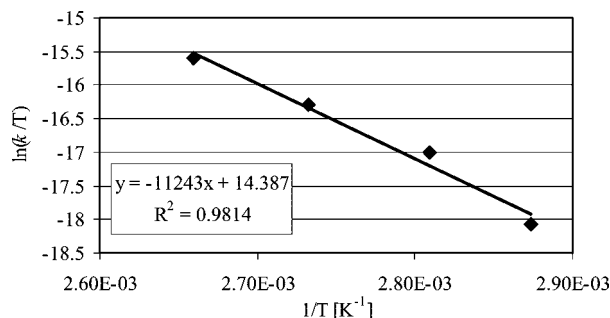


**Figure 8.** Eyring plot of the coupling of  $\text{TMSC}\equiv\text{CH}$  and  ${}^t\text{BuN}\equiv\text{C}$  by complex **1**.

from our conceptual questions regarding future new organo-5f-element reactivities.

**Temperature Influence on the Reaction Rate.** The influence of the temperature on the reaction rate was also investigated by repeating the same process at different temperatures (75, 85, 95, and 105 °C) with the concentrations of the catalyst, isonitrile, and alkyne kept constant. The following concentrations were used throughout the experiment: catalyst 0.028 M,  $\text{TMSC}\equiv\text{CH}$  1.260 M, and  ${}^t\text{BuN}\equiv\text{C}$  1.630 M.

The rate constant,  $k_{\text{obs}}$  ( $\text{M}\cdot\text{s}^{-1}$ ), was calculated at each temperature from the linear part of the plot showing the product concentration versus time. From the Arrhenius and Eyring equations, the thermodynamic parameters at the rate-determining step were calculated to be  $E_a = 23.1 \pm 0.3$  kcal/mol,  $\Delta H^\ddagger = 22.3 \pm 0.4$  kcal/mol, and  $\Delta S^\ddagger = -18.6 \pm 0.3$  eu (Figure 8).

This negative value of  $\Delta S^\ddagger$  points to a highly ordered transition state and corroborates that the rate-determining step goes via a three-centered transition state.

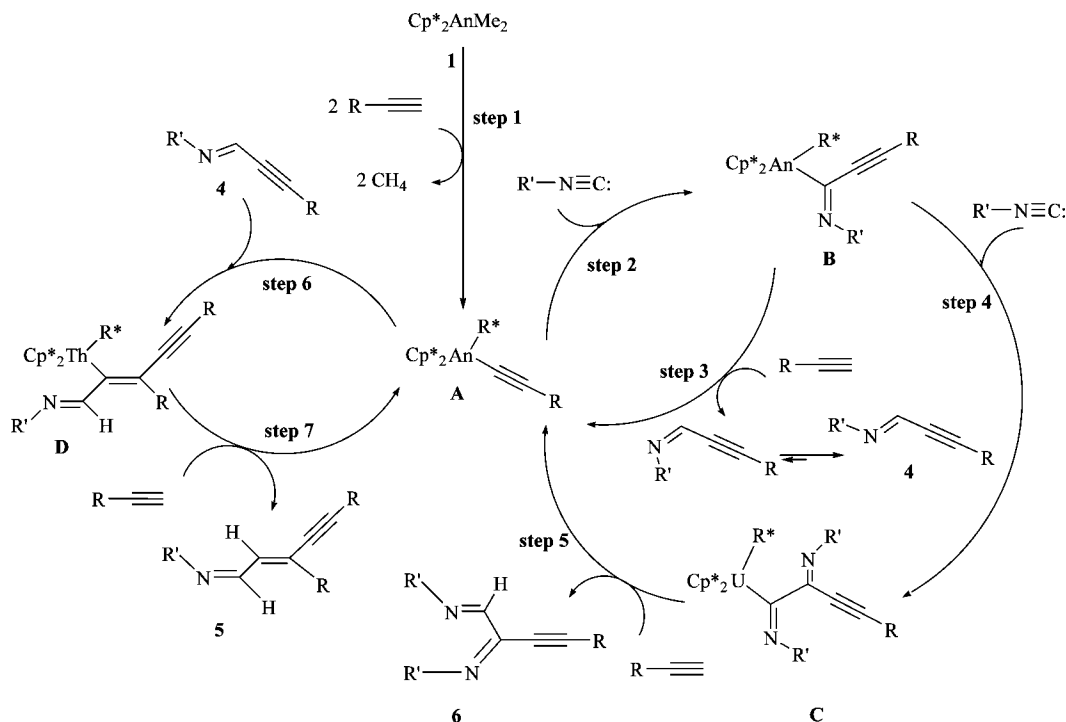
**Coupling of Terminal Alkynes and Isonitriles by  $\text{Cp}^*_2\text{ThMe}_2$ : Plausible Mechanism.** On the basis of the results presented earlier and the kinetics data we propose that the coupling reaction proceeds via the following mechanism, outlined in Scheme 2. The organoactinide complex **1** reacts with the terminal alkynes to yield the bis(acetylide) complex **A** (step 1). This complex undergoes a 1,1-insertion of the isonitrile into the metal–carbon bond to form the iminoacyl complex **B** (step 2) as the rate-determining step of the coupling reaction. The regiochemistry of this insertion locates the  $R'$  group of the isonitrile *syn* to the alkyne moiety due to the steric hindrance with the methyl groups of the cyclopentadienyl ring. At this stage it is not clear whether the second coordination site (marked as  $R^*$  in Scheme 2) undergoes similar reaction or remains as a spectator ligand. Protonolysis of **B** by an additional terminal alkyne (which is zero-order) yields the *Z*-monoinsertion product and regenerates complex **A** as the resting state in the catalytic cycle (step 3). This *Z* product will then isomerize to the more stable *E* isomer **4**. Under alkyne starvation conditions, this protonolysis step is not rapid, permitting the complex **B** to undergo an additional 1,1-insertion with a second isonitrile molecule to yield the corresponding intermediate **C** (step 4). The double-insertion product **6** is then obtained by the rapid protonolysis with a terminal alkyne (step 5) after the corresponding isomerization of the  $R'$  groups toward the more stable *E,E* isomer and regenerating the active bisacetylide complex **A**. With an excess of the nonbulky terminal alkynes, the bisacetylide complex **A** can react with product **4** to yield complex **D**, by insertion of the triple bond of **4** into the Th–acetylide bond (step 6). Protonolysis of **D** by another terminal alkyne yields product **5** and the active species **A** (step 7). To our knowledge, this is the first example of an insertion

of an internal triple bond into an actinide–carbon bond. As we have shown, the insertion of terminal alkynes into a metal acetylide bond produces either dimers or higher oligomers. However, when the reaction is performed in the presence of terminal and internal alkynes, only the products formed by the activation of the terminal alkyne are produced.<sup>2</sup> These results show that insertion of an internal triple bond must be higher in energy in comparison with that of the terminal alkynes. In contrast, the formation of compound **5** indicates that even in the presence of a terminal alkyne the insertion of the internal triple bond of **4** was preferred, presumably due to the electronic effects of the imine fragment ( ${}^t\text{BuN}=\text{C}-$ ), which induces a unique polarization of the internal triple bond. In addition, **4** inserts into the Th–acetylide bond in a selective fashion, with the imine fragment near the metal center; this suggests a weak interaction between the metal center and the imine nitrogen or the double bond, which enables the insertion of the internal triple bond.

The coupling reactions were also performed for comparison in the presence of complex **2** ( $\text{Cp}^*_2\text{U}\text{Me}_2$ ). Surprisingly, this complex catalyzed the formation of product **6** in addition to product **4** (eq 2 and Table 2, entries 1–6). As was monitored by NMR and GC/MS analysis, product **6** results from the coupling of one acetylene molecule with two isonitrile molecules. The ratio between the two products **4** and **6** was found to depend strongly on the bulkiness of the used alkyne. The bulky TMS moiety produced the monoinsertion product in 81% yield and the double-insertion compound in 19% yield after 48 h (Table 2, entry 2), whereas the use of the smaller moiety  ${}^i\text{Pr}$  increases the double-insertion product up to 50% yield (Table 2, entry 5). However, when the reaction was performed with an excess of  ${}^i\text{PrC}\equiv\text{CH}$ , the yield of **6** was reduced as a result of a fast protonation reaction, yielding the monoinsertion product **4** and the starting acetylide complex (Scheme 2, step 3). Hence, it was attractive to see the effect of the alkyne toward the formation of compound **6**. The effect of the alkyne  $R$  group on the ratio of products **4** and **6** is a consequence of the steric hindrance between the terminal alkyne  $R$  group and the isonitrile  $R'$  group of the last inserted unit that is disposed in a *Z* stereochemistry (see Scheme 2 complex **C**). The larger this steric interaction effect, the smaller the amount of complex **6** that will be produced.

When comparing these reactions with those performed with the thorium complex **1**, using equimolar amounts of alkyne and isonitrile, the thorium complex was found to be more reactive. For example, the reaction with relative proportions of **2**: ${}^t\text{BuN}\equiv\text{C}$ :  $\text{TMSC}\equiv\text{CH}$  = 1:100:100 produces in 24 h the organic products **4** and **6** in 67% and 3%, respectively, whereas for complex **1** this reaction is quantitative toward product **4**. As compared to either the corresponding thorium complex **1** or any other transition metal complex, the most remarkable feature of the organouranium complex **2** is its ability to perform in a one-pot reaction, yet not fully selectively, the coupling of two isonitrile molecules and one alkyne molecule. Important to point out, the same dependence of the substrates in the kinetics equation rate was found for the uranium complex **2** and thorium complex **1**.

One more issue that we wanted to study concerns the reactivity and/or the selectivity of neutral versus cationic complexes. For example, in the polymerization of olefins, neutral group IV complexes are not active, while the corresponding cationic complexes are extremely efficient. The same neutral/cationic effect was found in the oligomerization of cyclic esters.<sup>4b</sup> Hence, the very well defined cationic complex

**Scheme 2. Plausible Mechanism for the Catalytic Coupling of Isonitriles and Terminal Alkynes Mediated by  $\text{Cp}^*_2\text{AnMe}_2$  (An = Th, U) (for clarity we use  $\text{R}^*$  instead of  $\text{RC}\equiv\text{C}$ )****Table 2. Coupling of Terminal Alkynes ( $\text{RC}\equiv\text{CH}$ ) with Isonitriles ( $\text{R}'\text{N}\equiv\text{C}$ ) Catalyzed by Complexes 2 and 3**

entry	complex	$\text{R}'$	$\text{R}$	$\text{R}'\text{N}\equiv\text{C}$ : $\text{RC}\equiv\text{CH}^a$	time (h)	4 (%) <sup>b</sup>	6 (%) <sup>b</sup>
1	2	<sup>t</sup> Bu	TMS	100:60	6	56	13
2	2	<sup>t</sup> Bu	TMS	100:60	48	81	19
3	2	<sup>t</sup> Bu	Ph	100:150	6	65	7
4	2	<sup>t</sup> Bu	Ph	100:150	48	90	10
5	2	<sup>t</sup> Bu	<sup>i</sup> Pr	100:60	48	50	50
6	2	<sup>t</sup> Bu	<sup>i</sup> Pr	100:100	48	65	35
7	2	<sup>t</sup> Bu	<sup>i</sup> Pr	100:150	48	75	25
8	3	<sup>t</sup> Bu	TMS	100:100	4	40	
9	3	<sup>t</sup> Bu	TMS	100:100	12	80	
10	3	<sup>t</sup> Bu	Ph	100:100	12	81	
11	3	<sup>t</sup> Bu	<sup>i</sup> Pr	100:100	12	81	

<sup>a</sup> Relative to 1 equiv of catalyst. <sup>b</sup> Measured by <sup>1</sup>H NMR.

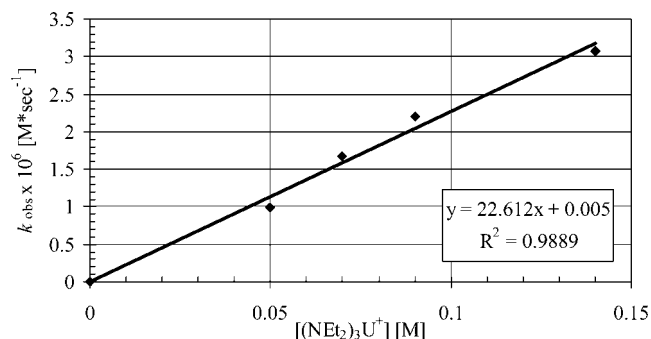
$[(\text{Et}_2\text{N})_3\text{U}][\text{BPh}_4]^{18}$  was used for comparison studies. The cationic complex  $[(\text{Et}_2\text{N})_3\text{U}][\text{BPh}_4]$  (3) produces the monoinsertion product 4 selectively with some minor byproduct such as the corresponding oligomers of the terminal alkynes.<sup>2a</sup> The yield of the product was found to have no dependence on the bulkiness of the R group of the different alkynes (Table 2, entries 7–10), indicating a plausible open, noncrowded, active species in which the ligand on the metal does not interfere much upon the approach of the  $\text{R}'$  group of the isonitrile. This effect related to an active species with an open coordination sphere was previously observed with a cationic complex during the production of the unexpected *cis* ene-yne isomer in the dimerization of terminal alkynes and was explained by an available vacant orbital.<sup>2d</sup> It was also shown that the amido groups of the cationic complex can be easily replaced with other amines, as well as terminal alkynes, as shown by the crystal structure of the complex obtained when using an excess of  $^t\text{BuNH}_2$ .<sup>2a</sup>

#### Kinetics Studies of the Coupling Reaction Catalyzed by Complex 3. Influence of the $[(\text{Et}_2\text{N})_3\text{U}][\text{BPh}_4]$ Concen-

tration on the Reaction Rate. Different concentrations of the catalyst were used while the alkyne and the isonitrile concentrations were kept constant. The kinetics of the coupling were monitored using the intensity changes in the substrate and product resonances over 3 or more half-lives. The rate constant,  $k_{\text{obs}}$  ( $\text{M}\cdot\text{s}^{-1}$ ), was calculated from the linear part of the plot, and the results are presented in Figure 9, showing that  $k_{\text{obs}}$  as a function of the catalyst concentration follows a first-order behavior.

**Influence of Isonitrile Concentration on the Reaction Rate.** In order to check the influence of the isonitrile concentration on the reaction rate, the concentration of  $^t\text{BuN}\equiv\text{C}$  was varied while the catalyst and alkyne concentrations were kept constant. The kinetics of the coupling reaction were monitored as described above, and the results are presented in Figure 10, indicating that the reaction is first-order in isonitrile.

**Influence of  $\text{TMSC}\equiv\text{CH}$  Concentration on the Reaction Rate.** In order to check the influence of alkyne concentrations on the reaction rate, the concentration of  $\text{TMSC}\equiv\text{CH}$  was varied, over a 10-fold range, while the catalyst and isonitrile concentrations were kept constant. As can be seen from Figure 11,  $k_{\text{obs}}$  as a function of the terminal alkyne concentration has

**Figure 9.** Dependence of  $k_{\text{obs}}$  on  $[(\text{Et}_2\text{N})_3\text{U}][\text{BPh}_4]$  concentration ([alkyne] = 1.0 M, [isonitrile] = 1.0 M, temp = 80 °C).

(18) Berthet, J. C.; Boisson, C.; Lance, M.; Vigner, J.; Nierlich, M.; Ephritikhine, M. *J. Chem. Soc., Dalton Trans.* **1995**, 301, 9–25.

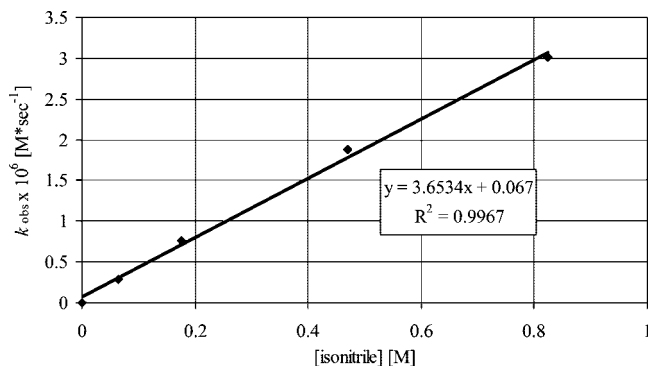


**Figure 10.** Dependence of  $k_{\text{obs}}$  on isonitrile concentration ([alkyne] = 1.0 M, [complex **3**] = 0.01 M, temp = 80 °C).

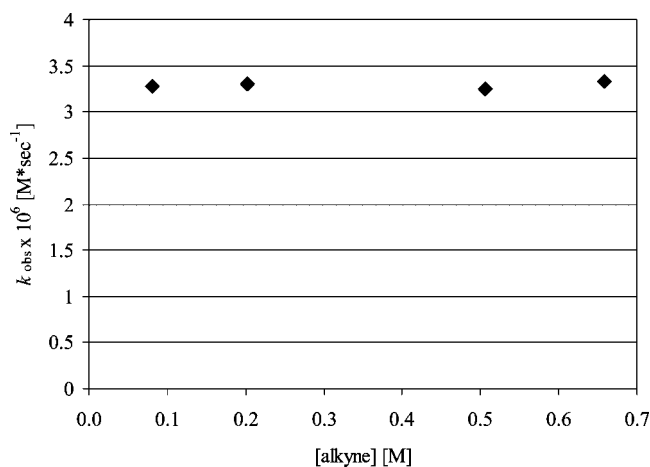


**Figure 11.** Dependence of  $k_{\text{obs}}$  on the  $\text{TMSCH}=\text{CH}$  concentration ([isonitrile] = 1.0 M, [complex **3**] = 0.01 M, temp = 80 °C).

a constant value of  $3.4 \times 10^{-6} \text{ (M} \cdot \text{s}^{-1})$ , indicating that zero-order kinetics were followed.

The combination of the kinetics data for the coupling of terminal alkynes and isonitriles catalyzed by the cationic complex **3** is presented in the general kinetics equation of the reaction (eq 5). This result leads to the conclusion that the rate-determining step in the coupling reaction with complex **3** (as with complexes **1** and **2**) is the insertion of the isonitrile into the metal–acetylide bond.

$$v = k[(\text{Et}_2\text{N})_3\text{U}^+][\text{t}^-\text{BuN}\equiv\text{C}][\text{TMSC}\equiv\text{CH}]^0 \quad (5)$$

**Temperature Influence on the Reaction Rate.** The influence of the temperature on the reaction rate was also investigated by repeating the same process at different temperatures (55, 70, 80, and 90 °C) with the concentrations of the catalyst, isonitrile, and alkyne kept constant. The following concentrations were used throughout the experiment: complex **3**, 0.070 M;  $\text{TMSC}\equiv\text{CH}$ , 1.011 M;  $\text{t}^-\text{BuN}\equiv\text{C}$ , 1.011 M.

The thermodynamic activation parameters were calculated to be  $E_a = 11.3 \pm 0.3 \text{ kcal/mol}$ ,  $\Delta H^\ddagger = 10.6 \pm 0.4 \text{ kcal/mol}$ , and  $\Delta S^\ddagger = -46.8 \pm 0.2 \text{ eu}$  (Figure 12).

On the basis of these kinetics results we can postulate that the coupling reaction promoted by complex **3** proceeds via a slightly different mechanism than observed for complex **1** or **2** (Scheme 3). The first step in the catalytic cycle is the fast equilibrium formation of the acetylide complex **E** with the concomitant reversible elimination of  $\text{Et}_2\text{NH}$ , followed by the rate-determining 1,1-insertion of the isonitrile. Protonolysis of complex **F** may be done by either  $\text{Et}_2\text{NH}$  or the terminal alkyne.

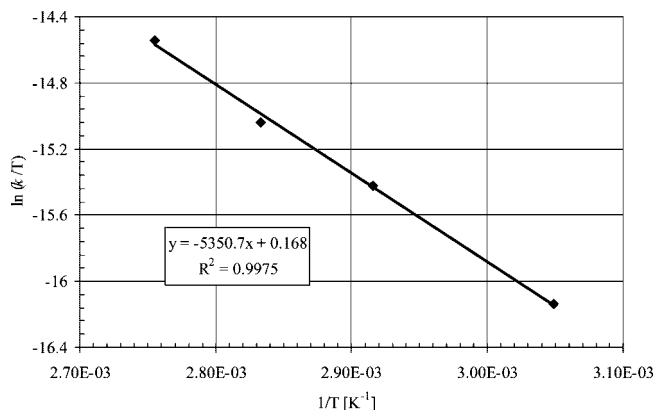
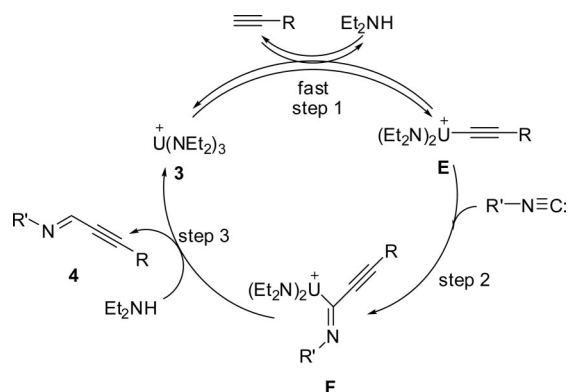


**Figure 12.** Eyring plot for the coupling of terminal alkynes and isonitrile catalyzed by complex **3**.

### Scheme 3. Plausible Mechanism for the Catalytic Coupling of Isonitriles and Terminal Alkynes Mediated by $[(\text{Et}_2\text{N})_3\text{U}][\text{BPh}_4]^a$



<sup>a</sup> In the presence of alkyne, isonitrile, product, or amine, the cationic complex is expected to be octahedrally coordinated.<sup>4,18</sup>

As we reported previously,  $\text{Et}_2\text{NH}$  is a harder base as compared to alkynes and hence tends to bind stronger to the hard uranium metal ion, causing a faster protonolysis to produce compound **4**.<sup>2b</sup> This alternative fast protonolysis process (step 3) produces the monoinsertion product **4** and the precatalyst  $[(\text{Et}_2\text{N})_3\text{U}][\text{BPh}_4]$  concomitantly. Moreover, this fast protonolysis prevents further insertions of isonitriles into **F**, which explains the absence of the double-insertion product when using  $[(\text{Et}_2\text{N})_3\text{U}][\text{BPh}_4]$  even in alkyne-starved conditions.

## Conclusions

In this contribution we have introduced a new chapter in the field of catalytic activity of organoactinide complexes. We have addressed conceptual questions concerning the reactivity of neutral/cationic organoactinide complexes in the catalytic reaction that include three-center transition states, by studying the coupling reaction between isonitriles and terminal alkynes.

We have found that the cationic complex  $[(\text{Et}_2\text{N})_3\text{U}][\text{BPh}_4]$  produces the *trans* monocoupling product between the isonitriles and the alkynes with trace amounts of the corresponding oligomers of the terminal alkynes. For the neutral  $\text{Cp}^*_2\text{UMe}_2$  complex, in addition to the monoinsertion, the double-insertion product of 2 equiv of isonitrile with 1 equiv of terminal alkyne was obtained. For the neutral  $\text{Cp}^*_2\text{ThMe}_2$  complex, also in addition to the monoinsertion, the double-insertion product of 2 equiv of alkyne with 1 equiv of isonitrile was obtained.

Kinetics studies showed that the reactions followed for the monocoupling formation a first-order dependence on catalyst and isonitrile and a zero-order dependence in alkyne, generating the general kinetic equation rate  $v = k[\text{catalyst}]^1[\text{isonitrile}]^1[\text{alkyne}]^0$ . Thermodynamic studies allowed us to calculate the energy of activation, in addition to the enthalpy and entropy of activation at the rate-determining step. These data show that the cationic complex is the more efficient catalyst, as compared to the thorium complex, with a lower enthalpy of activation ( $\Delta H^\ddagger = 10.6 \pm 0.4$  and  $22.3 \pm 0.4$  kcal/mol, respectively) and lower entropy of activation ( $\Delta S^\ddagger = -46.8 \pm 0.3$  and  $-18.6 \pm 0.3$  eu, respectively), presumably as a result of higher electrostatic interaction between the cationic complex and the carbene-like isonitrile. The tailoring of these coupling reactions with other substrates to develop a multicoupled process is under investigation.

## Experimental Section

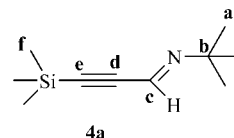
**Materials and Methods.** All manipulations of air-sensitive materials were performed with the rigorous exclusion of oxygen and moisture in flamed Schlenk-type glassware on a dual-manifold Schlenk line, or interfaced to a high-vacuum ( $10^{-5}$  Torr) line, or in a nitrogen-filled Vacuum Atmospheres glovebox with a medium-capacity recirculator (1–2 ppm  $\text{O}_2$ ). Argon and nitrogen were purified by passage through a MnO oxygen-removal column and a Davison 4 Å molecular sieve column. Hydrocarbon solvents THF- $d_8$ , benzene- $d_6$ , and toluene- $d_8$  were distilled under nitrogen from Na/K alloy. All solvents for vacuum line manipulations were stored in vacuo over Na/K alloy in resealable bulbs. The complexes  $\text{Cp}^*_2\text{AnMe}_2$  (An = Th, U)<sup>17</sup> and  $[(\text{Et}_2\text{N})_3\text{U}][\text{BPh}_4]$ <sup>18</sup> were prepared according to published methods.  $^t\text{BuNC}$ ,  $^i\text{PrNC}$ ,  $^n\text{PentNC}$ ,  $^t\text{BuC}\equiv\text{CH}$ ,  $^n\text{BuC}\equiv\text{CH}$ ,  $\text{TMSC}\equiv\text{CH}$ ,  $\text{PhC}\equiv\text{CH}$ , and  $^i\text{PrC}\equiv\text{CH}$  (Aldrich) were degassed and stored under nitrogen over molecular sieves (4 Å) and freshly vacuum-distilled before use.

NMR spectra were recorded on Avance 500 and Avance 300 Bruker spectrometers. Chemical shifts for  $^1\text{H}$  and  $^{13}\text{C}$  are referenced to internal solvent resonances and are reported relative to tetramethylsilane. All reactions monitored by NMR were performed in J. Young Teflon valve-sealed NMR tubes. GC/MS experiments were conducted in a GC/MS (Finnigan Magnum) spectrometer with a J&W DB5 column (30 m  $\times$  250  $\mu\text{m}$ ).

**Coupling of Terminal Alkynes and Isonitriles. General Procedure.** In a typical procedure, a J. Young NMR tube was charged in the glovebox with  $\text{Cp}^*_2\text{ThMe}_2$  (**1**) (5 mg, 0.009 mmol),  $\text{Cp}^*_2\text{UMe}_2$  (**2**) (7 mg, 0.013 mmol), or  $[(\text{Et}_2\text{N})_3\text{U}][\text{BPh}_4]$  (**3**) (7 mg, 0.009 mmol). Alkyne and  $^t\text{BuNC}$  at needed ratios and 0.5 mL of solvent ( $\text{C}_6\text{D}_6$  or  $\text{C}_7\text{D}_8$ ) were added by vacuum transfer on a high-vacuum line. The sealed tube was heated by means of an oil bath. The rapid darkening of the solution indicated the formation of the products. Monitoring of the reaction was done by  $^1\text{H}$  NMR. When the reaction went to completion, the products were identified by NMR and GC/MS analysis of the crude reaction mixture.

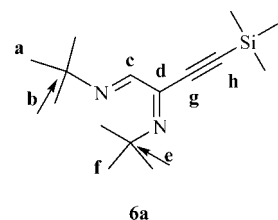
**Coupling of  $^t\text{BuNC}$  and  $\text{TMSC}\equiv\text{CH}$  with Complex 1.** According to the general procedure,  $\text{TMSC}\equiv\text{CH}$  (0.1 mL, 0.72 mmol or 0.2 mL, 1.44 mmol) and  $^t\text{BuNC}$  (0.08 mL, 0.7 mmol) were added and the reaction mixture was heated to 90 °C for 23 h to obtain product **4a** (R = TMS) (2-methyl-*N*-[3-(trimethylsilyl)prop-2-yn-1-ylidene]propan-2-amine) as the major product (85–90% yield relative to isonitrile in both cases).  $^1\text{H}$  NMR (500 MHz,  $\text{C}_6\text{D}_6$ ):  $\delta$  7.27 (s, 1H, c), 0.99 (s, 9H, a), 0.10 (s, 9H, f).  $^{13}\text{C}$  NMR (125 MHz,  $\text{C}_6\text{D}_6$ ):  $\delta$  139.6 (c), 103.8 (d), 96.1 (e), 58.8 (b), 29.2 (a), –0.3 (f). MS ( $m/z$ ): 182 [ $\text{MH}^+$ ].

**Coupling of  $^t\text{BuNC}$  and  $\text{TMSC}\equiv\text{CH}$  with Complexes 2 and 3.** According to the general procedure,  $\text{TMSC}\equiv\text{CH}$  (0.1 mL, 0.72 mmol) and  $^t\text{BuNC}$  (0.13 mL, 1.2 mmol) were added to the reaction mixture that contained complex **2**, and the mixture was



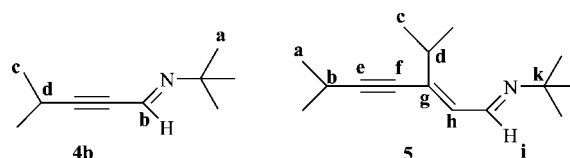
heated to 90 °C for 24 h to obtain product **4a** (R = TMS) (2-methyl-*N*-[3-(trimethylsilyl)prop-2-yn-1-ylidene]propan-2-amine) as the major product (81% yield) and **6a** (R = TMS) ([1-(*tert*-butylimino)-4-(trimethylsilyl)but-3-yn-2-ylidene]-2-methylpropan-2-amine) (19% yield). **6a**:  $^1\text{H}$  NMR (500 MHz,  $\text{C}_6\text{D}_6$ ):  $\delta$  7.84 (s, 1H, c), 1.44 (s, 9H, a), 0.96 (s, 9H, f), –0.04 (s, 6H, i).  $^{13}\text{C}$  NMR (125 MHz,  $\text{C}_6\text{D}_6$ ):  $\delta$  158.1 (c), 149.6 (d), 107.2 (g), 98.3 (h), 57.4 (b), 57.3 (e), 29.1 (a), 28.9 (f), –1.0 (i). MS ( $m/z$ ): 265 [ $\text{MH}^+$ ].

The same general procedure was applied with complex **3**. Accordingly,  $\text{TMSC}\equiv\text{CH}$  (0.16 mL, 1.25 mmol) and  $^t\text{BuNC}$  (0.10 mL, 0.90 mmol) were added, and the reaction mixture was heated to 90 °C for 48 h to obtain product **4a** as the major product (80% yield).



### Coupling of $^t\text{BuNC}$ and $^i\text{PrC}\equiv\text{CH}$ with Complex 1.

According to the general procedure,  $^i\text{PrC}\equiv\text{CH}$  (0.12 mL, 1.2 mmol) and  $^t\text{BuNC}$  (0.13 mL, 1.2 mmol) were added, and the reaction mixture was heated to 90 °C for 18 h to obtain product **4b** (R =  $^i\text{Pr}$ ) (2-methyl-*N*-[4-methylpent-2-yn-1-ylidene]propan-2-amine) as the major product (90% yield).  $^1\text{H}$  NMR (500 MHz,  $\text{C}_7\text{D}_8$ ):  $\delta$  7.34 (s, 1H, b), 2.43 (septet,  $J = 7$  Hz, 1H, d), 1.02 (s, 9H, a), 1.0 (d,  $J = 7$  Hz, 6H, c).  $^{13}\text{C}$  NMR (75 MHz,  $\text{C}_7\text{D}_8$ ) [a short relaxation time (2 s) was used so that the quaternary carbons were not observed]:  $\delta$  139.7 (b), 29.2 (a), 22.5 (c), 21.2 (d). GC-MS: (molecular weight 151)  $m/z$  152 ( $\text{M}^+ + \text{H}$ ), 136 ( $\text{M}^+ - \text{CH}_3$ ), 121 ( $\text{M}^+ - 2\text{CH}_3$ ), 106 ( $\text{M}^+ - 3\text{CH}_3$ ), 94 ( $\text{M}^+ - \text{C}_4\text{H}_9$ ). In a second experiment, a higher alkyne:isonitrile ratio was used ( $^i\text{PrC}\equiv\text{CH}$  (0.14 mL, 1.4 mmol) and  $^t\text{BuNC}$  (0.08 mL, 0.7 mmol)), and the reaction mixture was heated to 90 °C. After 17 h, product **4b** was obtained (95% yield) in addition to product **5** (5% yield, *N*-[3-isopropyl-6-methylhept-2-en-4-yn-1-ylidene]-2-methylpropan-2-amine). After 210 h, the ratio between **4b** and **5** was almost 1:1.  $^1\text{H}$  NMR (500 MHz,  $\text{C}_7\text{D}_8$ ):  $\delta$  8.59 (d, 1H,  $J = 8.9$  Hz, i), 6.53 (d, 1H,  $J = 8.9$  Hz, h), 2.52 (m, 2H,  $J = 7.1$ , b and d), 1.20 (s, 9H, j), 1.01 (d, 12H,  $J = 7.1$  Hz, a) 1.06 (d, 12H,  $J = 7.1$  Hz, c).  $^{13}\text{C}$  NMR (125 MHz,  $\text{C}_7\text{D}_8$ ) [a short relaxation time (2 s) was used so that the quaternary carbons were not observed]:  $\delta$  162.9 (i), 141 (h), 117 (g), 89.3 (f), 87.5 (e), 52.8 (k), 32.5 (j), 26.4 (d), 23.4 (b), 20.4 (a), 20.3 (c). MS: (molecular weight 219)  $m/z$  220 [ $\text{MH}^+$ ].

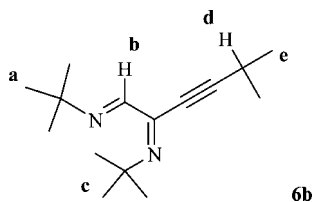


**Coupling of  $^t\text{BuNC}$  and  $^i\text{PrC}\equiv\text{CH}$  with Complexes 2 and 3.** According to the general procedure,  $^i\text{PrC}\equiv\text{CH}$  (0.1 mL, 0.6 mmol or 0.25 mL, 1.5 mmol) and  $^t\text{BuNC}$  (0.11 mL, 1.0 mmol) were added to the reaction mixture that contained complex **2** and heated to 90 °C for 48 h to obtain products **4b** (R =  $^i\text{Pr}$ ) (2-methyl-*N*-[4-methylpent-2-yn-1-ylidene]propan-2-amine) and **6b** ([1-(*tert*-butylimino)-5-methylhex-3-yn-2-ylidene]-2-methylpropan-2-



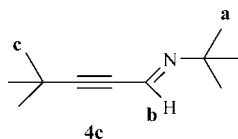
amine) in 1:1 and 3:1 ratio, respectively. **6b**:  $^1\text{H}$  NMR (500 MHz,  $\text{C}_7\text{D}_8$ ):  $\delta$  7.92 (s, 1H, **b**), 2.45 (septet, 1H,  $J = 7$  Hz, **d**), 1.56 (s, 9H, **a**), 1.07 (s, 9H, **c**), 1.04 (d, 6H,  $J = 7$  Hz, **e**).  $^{13}\text{C}$  NMR (125 MHz,  $\text{C}_7\text{D}_8$ ) [a short relaxation time (2 s) was used so that the quaternary carbons were not observed]:  $\delta$  160 (**b**), 30.9 (**a**), 30.8 (**c**), 23.4 (**e**), 23.1 (**d**). GC/MS:  $m/z$  235 ( $\text{MH}^+$ ).

The same general procedure was applied with complex **3**. Accordingly,  $^i\text{PrC}\equiv\text{CH}$  (0.18 mL, 1.12 mmol) and  $^i\text{BuN}\equiv\text{C}$  (0.10 mL, 0.90 mmol) were added and the reaction mixture was heated to 90 °C for 48 h to obtain product **4b** as major product (81% yield).



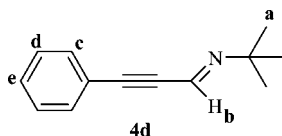
#### Coupling of $^i\text{BuNC}$ and $^i\text{BuC}\equiv\text{CH}$ with Complex 1.

According to the general procedure,  $^i\text{BuC}\equiv\text{CH}$  (0.06 mL, 0.5 mmol) and  $^i\text{BuN}\equiv\text{C}$  (0.08 mL, 0.5 mmol) were added and the reaction mixture was heated to 90 °C for 23 h to obtain **4c** ( $\text{R} = ^i\text{Bu}$ ), 2-methyl-*N*-(4,4-dimethylpent-2-ynylidene)propan-2-amine (90% yield).  $^1\text{H}$  NMR (500 MHz,  $\text{C}_6\text{D}_6$ ):  $\delta$  7.31 (s, 1H, **b**), 1.09 (s, 9H, **a**), 0.95 (s, 9H, **c**).  $^{13}\text{C}$  NMR (125 MHz,  $\text{C}_6\text{D}_6$ ) [a short relaxation time (2 s) was used so that the quaternary carbons were not observed]:  $\delta$  144.3 (**c**), 29.2 (**a**), 25.1 (**c**). MS ( $m/z$ ): 166 [ $\text{MH}^+$ ].



#### Coupling of $^i\text{BuNC}$ and $\text{PhC}\equiv\text{CH}$ with Complex 1.

According to the general procedure,  $\text{PhC}\equiv\text{CH}$  (0.1 mL, 1 mmol) and  $^i\text{BuN}\equiv\text{C}$  (0.12 mL, 1.05 mmol) were added and the reaction mixture was heated to 90 °C for 20 h to obtain **4d** ( $\text{R} = \text{Ph}$ ), 2-methyl-*N*-[3-phenylprop-2-yn-1-ylidene]propan-2-amine (89% yield).  $^1\text{H}$  NMR (300 MHz,  $\text{C}_7\text{D}_8$ ):  $\delta$  7.46 (s, 1H, **b**), 7.35 (m, 2H, **c**), 6.94 (m, 1H, **e**), 6.92 (m, 2H, **d**), 1.07 (s, 9H, **a**).

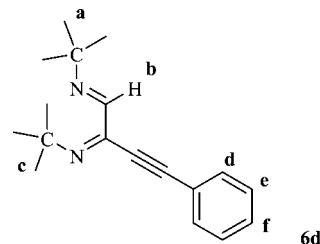


#### Coupling of $^i\text{BuNC}$ and $\text{PhC}\equiv\text{CH}$ with Complexes 2 and 3.

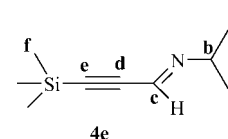
According to the general procedure,  $\text{PhC}\equiv\text{CH}$  (0.15 mL, 1.5 mmol) and  $^i\text{BuN}\equiv\text{C}$  (0.11 mL, 1.0 mmol) were added to the reaction mixture that contained complex **2** and heated to 90 °C for 48 h to obtain products **4d** ( $\text{R} = \text{Ph}$ ) (2-methyl-*N*-[3-phenylprop-2-yn-1-ylidene]propan-2-amine) as a major product (90% yield) and **6d** ([1-(*tert*-butylimino)-4-phenylbut-3-yn-2-ylidene]-2-methylpropan-2-amine) (10% yield). **6d**:  $^1\text{H}$  NMR (300 MHz,  $\text{C}_7\text{D}_8$ ):  $\delta$  7.98 (s, 1H, **b**), 7.35 (m, 2H, **d**), 6.94 (m, 1H, **f**), 6.92 (m, 2H, **e**), 1.58 (s, 9H, **a**), 1.14 (s, 9H, **c**). MS ( $m/z$ ): 268 [ $\text{MH}^+$ ].

The same general procedure was applied with complex **3**. Accordingly,  $\text{PhC}\equiv\text{CH}$  (0.09 mL, 0.90 mmol) and  $^i\text{BuN}\equiv\text{C}$  (0.10 mL, 0.90 mmol) were added and the reaction mixture was heated to 90 °C for 48 h to obtain product **4d** as major product (81% yield).

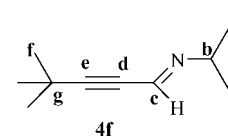
**Coupling of  $^i\text{PrNC}$  and  $\text{TMSC}\equiv\text{CH}$ .** According to the general procedure,  $\text{TMSC}\equiv\text{CH}$  (0.1 mL, 0.7 mmol) and  $^i\text{PrN}\equiv\text{C}$  (0.08 mL, 0.7 mmol) were added and the reaction mixture was heated to 90 °C for 4 h to obtain product **4e** ( $\text{R} = \text{TMS}$ ,  $\text{R}' = ^i\text{Pr}$ ) (*N*-(3-



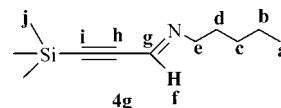
(trimethylsilyl)prop-2-ynylidene)propan-2-amine) as the *Z* isomer (84% yield). Longer heating times resulted in the isomerization of the product to the more stable *E* isomer.  $^1\text{H}$  NMR (*E* isomer, 500 MHz,  $\text{C}_6\text{D}_6$ ):  $\delta$  7.21 (s, 1H, **c**), 2.95 (m, 1H, **b**), 1.05 (d, 6H, **a**), 0.12 (s, 9H, **f**).  $^{13}\text{C}$  NMR (125 MHz,  $\text{C}_6\text{D}_6$ ):  $\delta$  141.7 (**c**), 102.1 (**d**), 93.1 (**e**), 55.2 (**b**), 25.4 (**a**), -0.2 (**f**). MS ( $m/z$ ): 168 [ $\text{MH}^+$ ].



**Coupling of  $^i\text{PrNC}$  and  $^i\text{BuC}\equiv\text{CH}$ .** According to the general procedure,  $^i\text{BuC}\equiv\text{CH}$  (0.12 mL, 1 mmol) and  $^i\text{PrN}\equiv\text{C}$  (0.11 mL, 1 mmol) were added and the reaction mixture was heated to 90 °C for 4 h to obtain product **4f** ( $\text{R} = ^i\text{Bu}$ ,  $\text{R}' = ^i\text{Pr}$ ), *N*-(4,4-dimethylpent-2-ynylidene)propan-2-amine (77% yield).  $^1\text{H}$  NMR (500 MHz,  $\text{C}_6\text{D}_6$ ):  $\delta$  7.33 (s, 1H, **c**), 3.05 (m, 1H, **b**), 1.15 (d, 6H, **a**), 1.02 (s, 9H, **f**).  $^{13}\text{C}$  NMR (125 MHz,  $\text{C}_6\text{D}_6$ ):  $\delta$  138.9 (**c**), 104.3 (**d**), 95.7 (**e**), 52.2 (**b**), 28.3 (**g**), 23.9 (**a**), 17.3 (**f**). MS ( $m/z$ ): 152 [ $\text{MH}^+$ ].

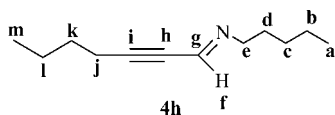


**Coupling of  $^i\text{PentNC}$  and  $\text{TMSC}\equiv\text{CH}$ .** According to the general procedure,  $\text{TMSC}\equiv\text{CH}$  (0.12 mL, 1 mmol) and  $^i\text{PentN}\equiv\text{C}$  (0.11 mL, 1 mmol) were added and the reaction mixture was heated to 90 °C for 0.5 h to obtain product **4g** ( $\text{R} = \text{TMS}$ ,  $\text{R}' = ^i\text{Pent}$ ), *N*-(3-(trimethylsilyl)prop-2-ynylidene)pentan-1-amine (95% yield) as a mixture of *E* and *Z* isomers. Longer heating times resulted in the complete isomerization to the *E* isomer.  $^1\text{H}$  NMR (500 MHz,  $\text{C}_6\text{D}_6$ ) *Z* isomer:  $\delta$  7.39 (t,  $J = 2.5$  Hz, 1H, **f**), 3.66 (t of d  $J = 2.5$ , 7 Hz, 2H, **e**), 1.59 (m, 2H, **d**), 1.23 (m, 4H, **b** + **c**), 0.79 (t, 3H, **a**), 0.06 (s, 9H, **j**). *E* isomer:  $\delta$  7.20 (t,  $J = 2.5$  Hz, 1H, **f**), 3.19 (t of d  $J = 2.5$ , 7 Hz, 2H, **e**), 1.49 (m, 2H, **d**), 1.13 (m, 4H, **b** + **c**), 0.74 (t, 3H, **a**), 0.06 (s, 9H, **j**).  $^{13}\text{C}$  NMR (125 MHz,  $\text{C}_6\text{D}_6$ ) *Z* isomer:  $\delta$  143.2 (**g**), 103.9 (**h**), 98.9 (**i**), 57.9 (**e**), 31.9 (**d**), 31.1 (**c**), 24.1 (**b**), 15.5 (**a**), 0.1 (**j**). *E* isomer:  $\delta$  145.2 (**g**), 104.3 (**h**), 97.0 (**i**), 64.0 (**e**), 31.0 (**d**), 30.3 (**c**), 23.3 (**b**), 15.1 (**a**), 0.1 (**j**).

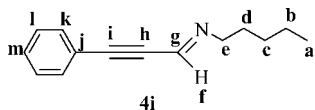


**Coupling of  $^i\text{PentNC}$  and  $^i\text{BuC}\equiv\text{CH}$ .** According to the general procedure,  $^i\text{BuC}\equiv\text{CH}$  (0.2 mL, 2 mmol) and  $^i\text{PentN}\equiv\text{C}$  (0.21 mL, 2 mmol) were added and the reaction mixture was heated to 90 °C for 5 h to obtain product **4h** ( $\text{R} = ^i\text{Bu}$ ,  $\text{R}' = ^i\text{Pentyl}$ ), *N*-(hept-2-ynylidene)pentan-1-amine (90% yield) as a mixture of *E* and *Z* isomers (with *Z*:*E* ratio of 2.4:1). After an additional 16 h at 90 °C partial isomerization of the *Z* isomer to the *E* isomer was observed (final *Z*:*E* ratio of 1:2.5).  $^1\text{H}$  NMR (500 MHz,  $\text{C}_6\text{D}_6$ ) *Z* isomer:  $\delta$  7.39 (s, 1H, **f**), 3.68 (t, 2H, **e**), 1.65 (m, 4H, **c** + **d**), 1.30–1.20 (m, 8H, **b**+**j**+**k**+**l**), 0.91 (t, 3H, **a**), 0.78 (t, 3H, **m**). *E*

isomer:  $\delta$  7.29 (s, 1H, **f**), 3.24 (t, 2H, **e**) 1.42 (m, 4H, **c** + **d**), 1.30–1.20 (m, 8H, **b** + **j** + **k** + **l**), 0.85 (t, 3H, **a**), 0.78 (t, 3H, **m**).  $^{13}\text{C}$  NMR (125 MHz,  $\text{C}_6\text{D}_6$ ) *Z* isomer:  $\delta$  143.6 (**g**), 100.3 (**h**), 97.8 (**i**), 57.6 (**e**), 34.6 (**d** or **j** or **k**), 32.3 (**d** or **j** or **k**), 31.1 (**d** or **j** or **k**), 22.2 (**c** or **l**), 22.8 (**c** or **l**), 16.1 (**b**), 14.9 (**a** or **m**), 14.1 (**a** or **m**). *E* isomer:  $\delta$  145.6 (**g**), 104.3 (**h**), 97.0 (**i**), 63.8 (**e**), 33.5 (**d** or **j** or **k**), 31.7 (**d** or **j** or **k**), 30.3 (**d** or **j** or **k**), 24.3 (**c** or **l**), 23.2 (**c** or **l**), 15.9 (**b**), 15.5 (**a** or **m**), 13.1 (**a** or **m**).



**Coupling of "PentNC with  $\text{PhC}\equiv\text{CH}$ .** According to the general procedure,  $\text{PhC}\equiv\text{CH}$  (0.1 mL, 1 mmol) and "PentNC" (0.12 mL, 1.05 mmol) were added and the reaction mixture was heated to 90 °C for 5 h to obtain **4i** ( $R = \text{Ph}$ ), *N*-(3-phenylprop-2-ynylidene)pentan-1-amine (89% yield).  $^1\text{H}$  NMR (300 MHz,  $\text{C}_7\text{D}_8$ ):  $\delta$  7.43 (s, 1H, **f**), 7.41 (m, 2H, **k**), 7.25 (m, 2H, **l**), 6.92 (m, 1H, **m**), 3.59 (t, 2H, **e**) 1.68 (m, 4H, **c** + **d**), 1.14 (m, 2H, **b**), 0.87 (t, 3H, **a**).



**Kinetics Study of the Coupling of  $\text{TMSC}\equiv\text{CH}$  and "BuNC by Complex 1.** In a typical experiment, a 5 mm NMR tube with a Teflon valve (previously flamed under vacuum) was charged in the glovebox with  $\text{Cp}_2^*\text{ThMe}_2$  (2–20 mg, 0.0037–0.0375 mmol as a solution in benzene- $d_6$ ),  $\text{TMSC}\equiv\text{CH}$  (0.02–0.2 mL, 0.14–1.4 mmol), and "BuNC" (0.015–0.15 mL, 0.14–1.4 mmol). Benzene- $d_6$  was then added to bring the total volume of the solution to 0.7 mL. The tube was closed, quickly removed from the glovebox, and maintained at 0 °C until NMR measurements were initiated. The sample was quickly warmed and inserted into the probe, and an initial spectrum was recorded. After recording the spectrum at each time interval the tube was removed from the probe and kept at the required temperature by means of an oil bath. Data were acquired using eight scans per time interval sequence. The kinetics were monitored by the appearance of the coupling product resonances of the TMS group and the imine hydrogen ( $\delta$  0.10 and 7.27 ppm, respectively) over 3 half-lives. The concentration of the coupling product at time  $t$  ( $C$ ) was determined from the area of the  $^1\text{H}$ -normalized integrals of product standardized to the total area

of resonances of the TMS groups in the product and the starting  $\text{TMSC}\equiv\text{CH}$  ( $\delta$  0.05 ppm). This sum remains constant and equal to the initial concentration of  $\text{TMSC}\equiv\text{CH}$  ( $t = 0$ ) during the entire reaction process. All the data collected could be convincingly fit ( $R > 0.98$ ) by least-squares to the kinetic equations I and II where  $C_0$  is the initial concentration of the substrate.

$$\log(C/C_0) = mt \quad (\text{I})$$

$$\frac{1}{C} = \frac{1}{C_0} + mt \quad (\text{II})$$

The ratio of catalyst to substrate was accurately measured by calibration with internal standards. Turnover frequencies ( $N_t$ ,  $\text{h}^{-1}$ ) were calculated from the least-squares-determined slopes ( $m$ ) of the resulting plots.

**Kinetics Study of the Coupling of  $\text{TMSC}\equiv\text{CH}$  and "BuNC by Complex 3.** In a typical experiment, a 5 mm NMR tube with a Teflon valve (previously flamed under vacuum) was charged in the glovebox with  $[(\text{Et}_2\text{N})_3\text{U}][\text{BPh}_4]$  (5–16 mg, 0.0068–0.0206 mmol as a solution in benzene- $d_6$ ),  $\text{TMSC}\equiv\text{CH}$  (0.008–0.06 mL, 0.05–0.42 mmol), and "BuNC" (0.008–0.065 mL, 0.071–0.575 mmol). Benzene- $d_6$  was then added to bring the total volume of the solution to 0.7 mL. The tube was closed, quickly removed from the glovebox, and maintained at 0 °C until NMR measurements were initiated. The sample was quickly warmed and inserted into the probe, and an initial spectrum was recorded. After recording the spectrum at each time interval the tube was removed from the probe and kept at the required temperature by means of an oil bath. Data were acquired using eight scans per time interval sequence. The kinetics were monitored by the appearance of the coupling product resonances of the TMS group and the imine hydrogen ( $\delta$  0.10 and 7.27 ppm, respectively) over 3 half-lives. The concentration of the coupling product at time  $t$  ( $C$ ) was determined from the area of the  $^1\text{H}$ -normalized integrals of product standardized to the total area of resonances of the TMS groups in the product and the starting  $\text{TMSC}\equiv\text{CH}$  ( $\delta$  0.05 ppm). This sum remains constant and equal to the initial concentration of  $\text{TMSC}\equiv\text{CH}$  ( $t = 0$ ) during the entire reaction process. All the data collected could be convincingly fit ( $R > 0.98$ ) by least-squares to the kinetic equations I and II, where  $C_0$  is the initial concentration of substrate.

**Acknowledgment.** This research was supported by the Israel Science Foundation Administered by the Israel Academy of Science and Humanities under Contract 83/01-1. We want to thank Dr. Manab Sharma for the scientific discussions.

OM701223X